Decoupling Charge Transport and Electroluminescence in a High Mobility Polymer Semiconductor

*David J. Harkin, Katharina Broch, Maximilian Schreck, Harald Ceymann, Andreas Stoy, Chaw-Keong Yong, Mark Nikolka, Iain McCulloch, Natalie Stingelin, Christoph Lambert, and Henning Sirringhaus**

Over the past decade the electrical performance of solution processed polymer semiconductors has increased immensely, in particular low bandgap donor–acceptor structures have realized hole and electron mobilities greater than that found in amorphous silicon.[1,2] However, one of the major outstanding challenges is to develop material systems which simultaneously display balanced and high ambipolar charge carrier mobility whilst retaining a high fluorescence quantum yield (FQY).[3] It is sometimes argued that the strong intermolecular interactions that are needed to achieve a high carrier mobility lead to inefficient fluorescence due to formation of nonemissive intermolecular excited states. However, there is no rigorous, general scientific argument why high mobility and high FQY are mutually exclusive in organic materials.[4,5] To date the best compromize between mobility and light emission has been found in a range of oligophenylenethiophene single crystals.[6,7] This material class has presented FQYs of up to 0.8 as well as electron and hole mobilities on the order of 1 and 0.1 $cm^2\ V^{-1}\ s^{-1}$, respectively.[8] Very recently a small molecule 2,6-diphenylanthracene has been reported to possess hole mobilities of 34 $cm^2\ V^{-1}\ s^{-1}$ as well as a FQY of 0.41 and was integrated into both organic light emitting diodes (OLEDs) and field effect transistors (FETs).[9] Notwithstanding, these systems suffer from the processing constraints of single crystal growth and are thus not applicable for large scale solution processing. On the other hand, state-of-the art, high mobility polymer semiconductors with carrier mobilities often exceeding 1 $cm^2\ V^{-1}\ s^{-1}$ overwhelmingly exhibit low FQYs. This has been a major limitation for the development of high brightness electroluminescent devices, such as an electrically injected laser diode and is due to a number of quenching mechanisms inherent to the current design principles of these systems.[3] The most fundamental of these mechanisms is the Energy Gap Law, which describes an increase in the rate of internal conversion as the optical bandgap of a chromophore decreases in energy.[10,11] However, to achieve high charge carrier mobilities a low intrachain disorder is favorable, which results in a long exciton delocalization and therefore a low bandgap.[12,13] Moreover, the donor–acceptor structure of these systems further reduces the optical bandgap and also results in a polar backbone which undergoes strong dipole–dipole interactions in the solid state, quenching fluorescence.[14,15] In addition to this, solid state chain interactions can lead to the formation of interchain charge-transfer states, which have lower oscillator strengths than their Frenkel counterparts and can therefore also lead to fluorescence quenching.[5] In order to take advantage of the recent progress in high mobility polymers and to use these record-breaking high mobility materials in efficient, high brightness light emitting devices, ways have to be found to increase their FQY without negatively impacting the charge transport.

In this paper, we demonstrate a method to decouple electrical performance and electroluminescence using efficient resonance energy transfer (RET) from a high mobility polymer to a highly emissive near-infrared (NIR) squaraine dye oligomer. Choosing donor–acceptor combinations with energetics favorable to a fast energy transfer rate allows the use of low acceptor concentrations which does not significantly impact charge carrier mobility. In doing so we were able to increase the external quantum efficiency (EQE) by almost an order of magnitude without detrimentally impacting the current density and field effect mobility. We thus realized high brightness NIR OLEDs with radiances up to 5 $W\ m^{-2}\ str^{-1}$ at 800 nm which is a wavelength of interest for polymer optical fibres and biomedical imaging.[16,17] This brightness rivals cutting edge, high brightness solution processed inorganic NIR LEDs.[15,18–25] For example, recent research into solution processed perovskite devices has yielded the brightest and most efficient solution processed NIR LEDs reported to date with radiances of 28 $W\ m^{-2}\ str^{-1}$ at 760 nm using $CH_3NH_3PbI_3$_xClx as the emissive component.[22] This was achieved by careful control of the interfacial energetics using polyethylenimine as a surface modification for a zinc oxide nanocrystal electron injection layer. Quantum dots, on the other hand, have achieved NIR

D. J. Harkin, Dr. K. Broch, Dr. C.-K. Yong, Dr. M. Nikolka, Prof. H. Sirringhaus
Department of Physics
University of Cambridge
Cambridge CB3 0HE, UK
E-mail: HS220@cam.ac.uk
M. Schreck, H. Ceymann, A. Stoy, Prof. C. Lambert
Institut für Organische Chemie
Universität Würzburg
97074 Würzburg, Germany
Prof. I. McCulloch
Department of Chemistry
Imperial College London
London SW7 2AZ, UK
Prof. N. Stingelin
Department of Materials
Imperial College London
London SW7 2AZ, UK

DOI: 10.1002/adma.201600851

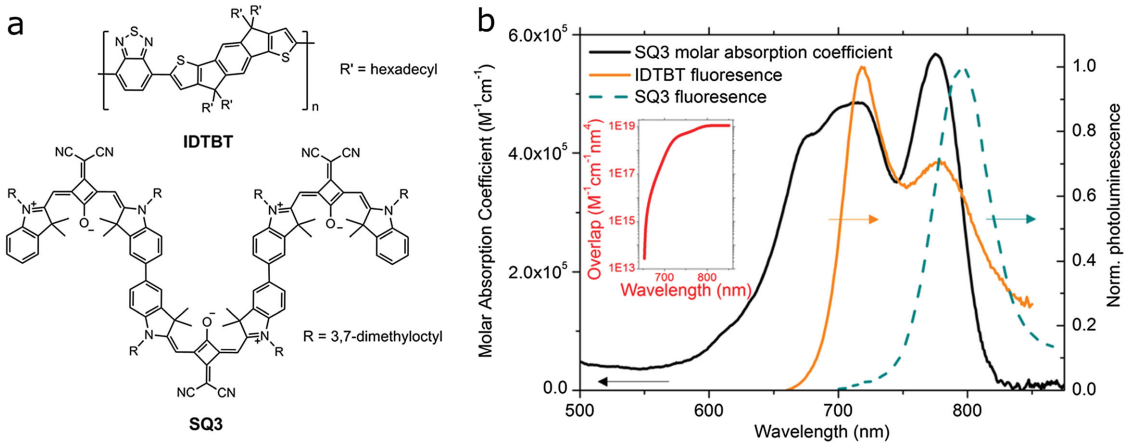

Figure 1. Structure and spectral overlap of IDTBT and SQ3. a) Chemical structure of IDTBT (top) and SQ3 (bottom) chromphore. b) IDTBT fluorescence spectrum with molar absorption and fluorescence spectra of SQ3 in o-DCB showing the high spectral overlap between the two molecules of which the cumulative value is quantified in the inset.

brightness up to 6 W m^{-2} str^{-1} but are currently limited by a number of quenching of mechanisms at high current densities such as Auger recombination.[19,26] Recently quantum dot-perovskite nanohybrids have been synthesized which combine the good electrical transport of organohalide perovskite crystalline solids with the efficient near-infrared emission of quantum dots in a similar concept to the work demonstrated here.[27] The efficient energy transfer in this system is mediated by the long exciton diffusion length apparent in perovskite films, which can be 2 orders of magnitude larger than that generally found in polymeric semiconductors.[28,29] This further illustrates the need for efficient RET in the organic semiconducting system presented here to compensate for the relatively short exciton diffusion length.

RET is a long range dipole coupling process whereby a donor molecule can transfer its excitation to an energetically suitable acceptor molecule.[30] RET acts over distances in the range of 1–10 nm and its efficiency is strongly correlated to the donor–acceptor spacing, donor FQY and the spectral overlap between the donor fluorescence spectrum and the acceptor absorption spectrum.[31–34] The metric used to describe the coupling strength between two chromophores is known as the Förster radius (R_0) and defines the donor–acceptor spacing at which energy transfer is equally likely as decay of the excited donor molecule. R_0 can be determined in a randomly orientated medium using the expression

$$R_0 = 0.197\left(n^{-4}\phi_D J(\lambda)\right)^{1/6} \quad (1)$$

where R_0 is in units of Å, n is the refractive index of the medium, ϕ_D is the FQY of the donor molecule in the absence of the acceptor.[31] $J(\lambda)$ is the spectral overlap between the fluorescence of the donor and the absorption of the acceptor in units of $m^{-1}cm^{-1}nm^4$. For stationary donor and acceptor molecules the exciton transfer efficiency is given by

$$\gamma = \frac{R_0^6}{R_0^6 + r^6} \quad (2)$$

where r is the donor–acceptor spatial separation. Owing to the low FQY present in high mobility polymer systems it was established that high values of R_0 could be attainable only through maximizing the spectral overlap with the acceptor molecule.

Recently, our group demonstrated the exceptionally low intrachain disorder in the high mobility polymer poly(indacenodithiophene-*alt*-benzothiadiazole) (IDTBT, **Figure 1**a) which is due to its backbone conformation being disorder tolerant.[12] In fact while it has been reported that films of IDTBT annealed at 150 °C show weak long range order we find that neat unannealed films show no long range order in grazing incidence wide angle X-ray scattering despite possessing hole mobilities of around 1.5 cm^2 V^{-1} s^{-1} (Supporting Information).[35] We chose this polymer as a suitable transport medium because of its high mobility in transistor structures at room temperature, high solubility (<120 mg mL^{-1} 1,2 dichlorobenzene) and the mentioned lack of long range structural order which was expected to facilitate incorporation of acceptor molecules without negatively effecting the charge transport.[35,36] When solvated in 1,2 dichlorobenzene, the FQY of neat IDTBT is 0.18 with an exciton lifetime of 1.3 ns. However in the thin film the FQY drops to 0.02 and the lifetime to around 90 ps which suggests strong nonradiative quenching in the solid state (Supporting Information) speculated to be the formation of nonemissive interchain excited states.[5] In thin films IDTBT exhibits a NIR fluorescence peak at 718 nm as shown in Figure 1b and has a highest occupied molecular orbital (HOMO) and lowest unoccupied molecular orbital (LUMO) of −5.3 eV and −3.6 eV, respectively, as reported previously.[37] This demonstrates the long exciton delocalization and/or stronger donor substitution for IDTBT in comparison to structurally similar polymers such as poly(9,9-dioctylfluorene-*alt*-benzothiadiazole) (F8BT) which displays a peak fluorescence of 540 nm, a FQY of 0.6 but a mobility which is lower by a factor of 100.[38] Owing to the relatively low bandgap of IDTBT the choice of a suitable acceptor molecule for efficient RET was challenging because until recently there was little evidence of organic systems which displayed efficient emission in the NIR. For example, the prototypical NIR laser dye 1,1′,3,3,3′,3′-hexam

ethylindotricarbocyanine iodide with an emission maximum of 730 nm exhibits a FQY of up to 0.3 in very dilute solution, and drops significantly in higher concentrations due to molecular aggregation (Supporting Information).[39] On the other hand, the use of quantum dots as an emissive component is an interesting approach and has been successfully demonstrated in a number of systems.[19,20,40] However, the volume ratios required are up to 50% due to the significantly larger diameter of a quantum dot in comparison to an organic dye molecule. This is expected to impinge upon charge transport and therefore is not ideally suited for the purposes of this study.

Recently, low bandgap squaraine dyes with high FQYs have been reported and have been successfully demonstrated in light emitting organic devices.[33,41,42] Moreover, due to their remarkable molar absorption coefficients (>10^5 M^{-1} cm^{-1}) they have been used to realize highly efficient RET in systems where the donor is weakly emissive.[34,43] Therefore, this material class offers the possibility to use ultralow concentrations of acceptor materials as the emissive component.

Ter[bis(indolenine)dicyanomethylensquaraine] (SQ3) is a recently synthesized squaraine dye trimer (Figure 1a and Supporting Information) which has absorption characteristics ideally suited for efficient resonance energy transfer from IDTBT (Figure 1b) and a high FQY of 0.58 (0.20) in toluene ($CHCl_3$). SQ3 exhibits a maximum molar absorption coefficient of 5.5×10^5 M^{-1} cm^{-1} at a wavelength of 780 nm in o-dichlorobenzene (DCB) and overlaps strongly with the fluorescence spectra of IDTBT. The integrated spectral overlap was found to be 1.2×10^{17} M^{-1} cm^{-1} nm^4. Using Equation (1) with an IDTBT FQY of 0.02 and an average refractive index of 2, determined by spectroscopic ellipsometry (Supporting Information), the Förster radius was calculated to be 4.5 nm. This is a large Förster radii for a solid state organic system despite the very low FQY of neat IDTBT thin films.[32–34] As there is little solvatochromic spectral shift in SQ3 (Supporting Information) we believe that it is reasonable to assume a similar absorption spectrum when solvated in DCB and IDTBT. The HOMO and LUMO of SQ3 were determined by cyclic voltammetry and found to be −5.32 and −3.70 eV, respectively (Supporting Information).

In order to study the photophysics of the system we prepared spin coated films of IDTBT blended with small concentrations of SQ3. The films were not annealed as heating was found to dramatically decrease the energy transfer efficiency, most probably due to loss of molecular mixing in the blend film. **Figure 2**a shows the photoluminescence spectra of SQ3/IDTBT blend films with mass ratios of 0.025, 0.075, 0.3 wt. % as well as the neat film. It can be seen that the 795 nm SQ3 emission peak increases with increased dye loading. The absorption spectra (Figure 2a inset), on the other hand, show no change even at a dye loading of 0.3 wt. %. This observed increase in fluorescence from the SQ3 component without change in the absorption spectrum indicates a strong energy transfer process occurring in the film. To confirm that this was in fact an energy transfer process and not direct excitation of the SQ3, photoluminescence excitation measurements were performed on neat IDTBT, solvated SQ3 as well as the 0.3 wt. % SQ3 blend, shown in Figure 2b. It can be seen that the 795 nm fluorescence component in the blend film follows the excitation of the IDTBT component rather than the solvated SQ3. This confirms that it is in fact the IDTBT component, which absorbs the incident photon and subsequently steps its excitation to the SQ3. To further investigate the energy transfer process, time resolved fluorescence measurements were carried out on neat IDTBT as well as SQ3 doped films. The fluorescence decay of the 740 nm IDTBT component as a function of time after excitation is plotted in Figure 2c. It can be seen that the exciton lifetime shortens as the SQ3 concentration is increased, consistent with a deactivating energy transfer process. The fluorescence decays can be fitted with monoexponential models from which the exciton lifetimes can be extracted. The exciton lifetime of the neat IDTBT film was found to be 90 ps, which decreased to 25 ps in the film loaded with 1 wt. % SQ3, as illustrated in the inset. The energy transfer efficiency was calculated using the drop in peak IDTBT fluorescence intensity and the equation

$$\gamma = 1 - \frac{I_{DA}}{I_D} \tag{3}$$

where γ is the energy transfer efficiency, I_{DA} is the IDTBT fluorescence intensity in the presence of SQ3, and I_D is the fluorescence intensity of neat IDTBT.[33] This was further confirmed using the time resolved fluorescence study and the equation

$$\gamma = 1 - \frac{\tau_{DA}}{\tau_D} \tag{4}$$

where τ_{DA} and τ_D are the respective lifetimes of the blend and neat films, respectively. Figure 2d shows the energy transfer efficiency as a function of SQ3 concentration. It can be seen that even at low concentrations the process is efficient, reaching a value of 0.5 at a SQ3 loading of 0.3 wt. %. This is the first demonstration of highly efficient energy transfer from a high mobility polymer to an acceptor compound.

In order to determine whether this energy transfer process resulted in a fluorescence enhancement, FQY measurements were carried out. Figure 2e shows the FQY and relative integrated photoluminescence intensity of the blend films as a function of SQ3 concentration. It can be seen that the FQY reaches a peak of 0.077 which is a threefold enhancement with respect to the neat IDTBT and is among the highest FQYs reported for solid state organic systems which emit in the NIR and similar to that of the recently reported dot-in-perovskite solids.[17,37] The FQY and fluorescence enhancement then plateaus and drops off as the concentration is further increased. Assuming that the FQY of SQ3 in dilute solution is constant as a function of SQ3 concentration, the total theoretical FQY should be 0.29 at a loading of 0.3 wt. %, using the equation $\phi_{blend} = \phi_{ISQ}\,\gamma + \phi_{IDTBT}(1-\gamma)$ where ϕ_{blend}, ϕ_{ISQ}, ϕ_{IDTBT} are the FQYs of the overall blend film, solvated SQ3, and IDTBT, respectively. This is a factor of 4 higher than the value measured for the blend film. SQ3 in the solid state however, drop casted from a 1 mg mL^{-1} solution in DCB, was found to have significantly reduced fluorescence below the sensitivity of our measurement techniques. Therefore, aggregation between SQ3 molecules is a likely rational for the limitation in fluorescence in the blend film. This is further evidenced by a red shift in the SQ3 fluorescence spectrum.

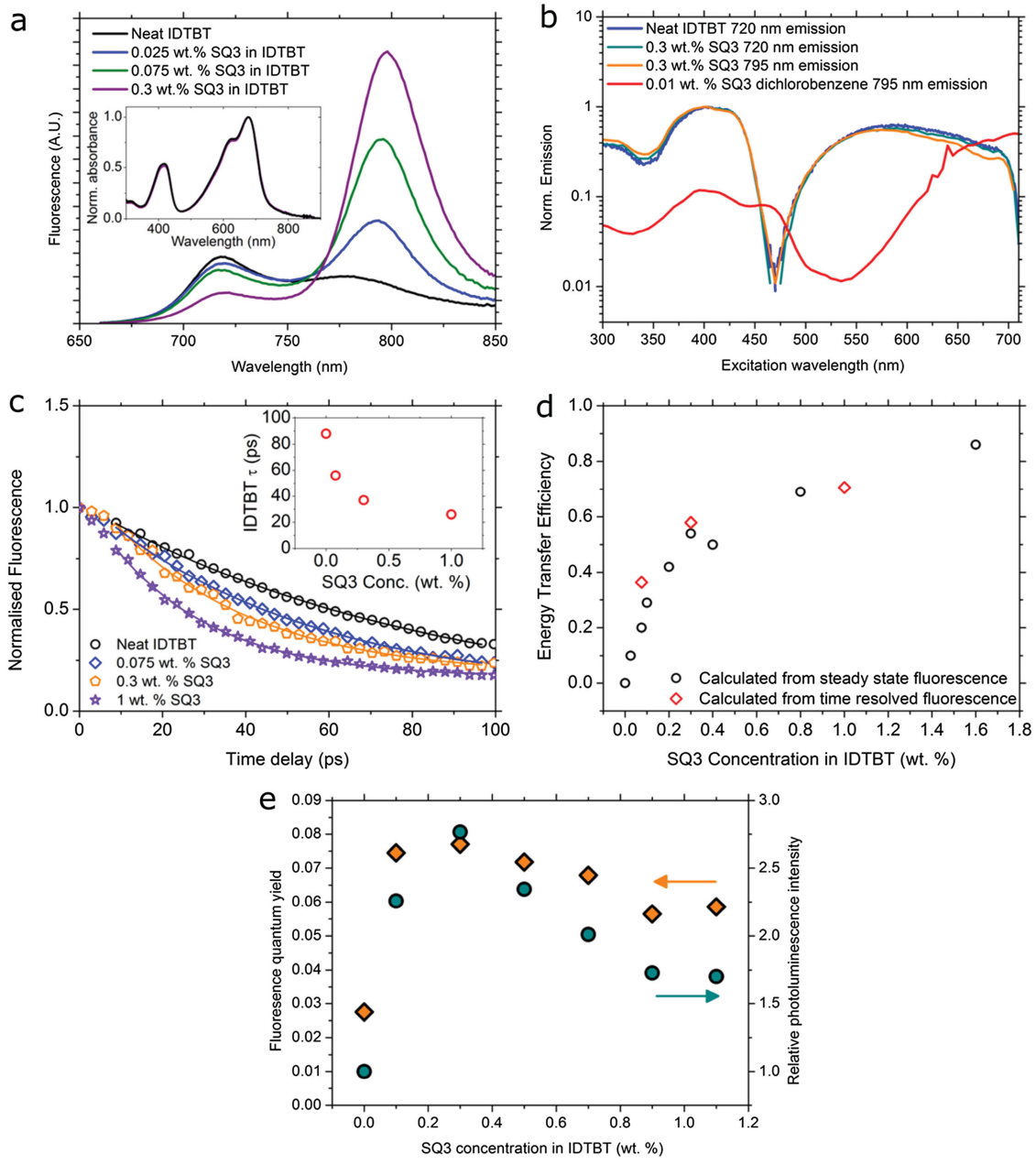

Figure 2. The photophysics of IDTBT-SQ3 blend films. a) The photoluminescence spectra of neat IDTBT as well as films blended with low concentrations of SQ3. It can be seen that the intensity of the 720 nm IDTBT component drops as the SQ3 concentration is increased. This is complemented by a strong increase in the SQ3 component which has a higher FQY than IDTBT. The inset shows the absorption spectrum of neat IDTBT as well as that of a film doped with 0.3 wt. % SQ3, illustrating that adding SQ3 in such low concentrations has no effect on the absorption of the blend system. b) Photoluminescence excitation spectra of a neat IDTBT film, solvated SQ3 as well as the IDTBT and SQ3 components in a 0.3 wt. % blend film. The fluorescence of the 795 nm SQ3 component in the blend film follows that of the neat IDTBT film at 720 nm which demonstrates that excitation of the SQ3 is through an energy transfer process rather than direct. c) The fluorescence decay of the 700 nm component of neat IDTBT and IDTBT blended with SQ3 fitted with monoexponential decays of which the decay constant is plotted in the inset. d) The exciton transfer efficiency from IDTBT to SQ3 as a function of SQ3 concentration. The transfer process is very efficient even at low SQ3 concentrations as for example an efficiency of 0.5 is achieved at a loading of 0.3 wt. %. e) The measured FQY and relative photoluminescence intensity of the IDTBT-SQ3 blend films. The FQY and relative fluorescence enhancement peaks at a dye loading of 0.3 wt. % after which it decreases due to the molecular aggregation.

In order to study further the dynamics of the energy transfer process time resolved fluorescence was utilized to decouple the IDTBT and SQ3 populations. Time resolved fluorescence was carried out measuring at 740 and 800 nm corresponding to the IDTBT as well as the IDTBT + SQ3 convolved signal respectively. **Figure 3**a–c shows the extracted time resolved population data for the IDTBT and SQ3 components for dye loadings of 0.075, 0.3, and 1 wt. %, respectively. It can be seen that while

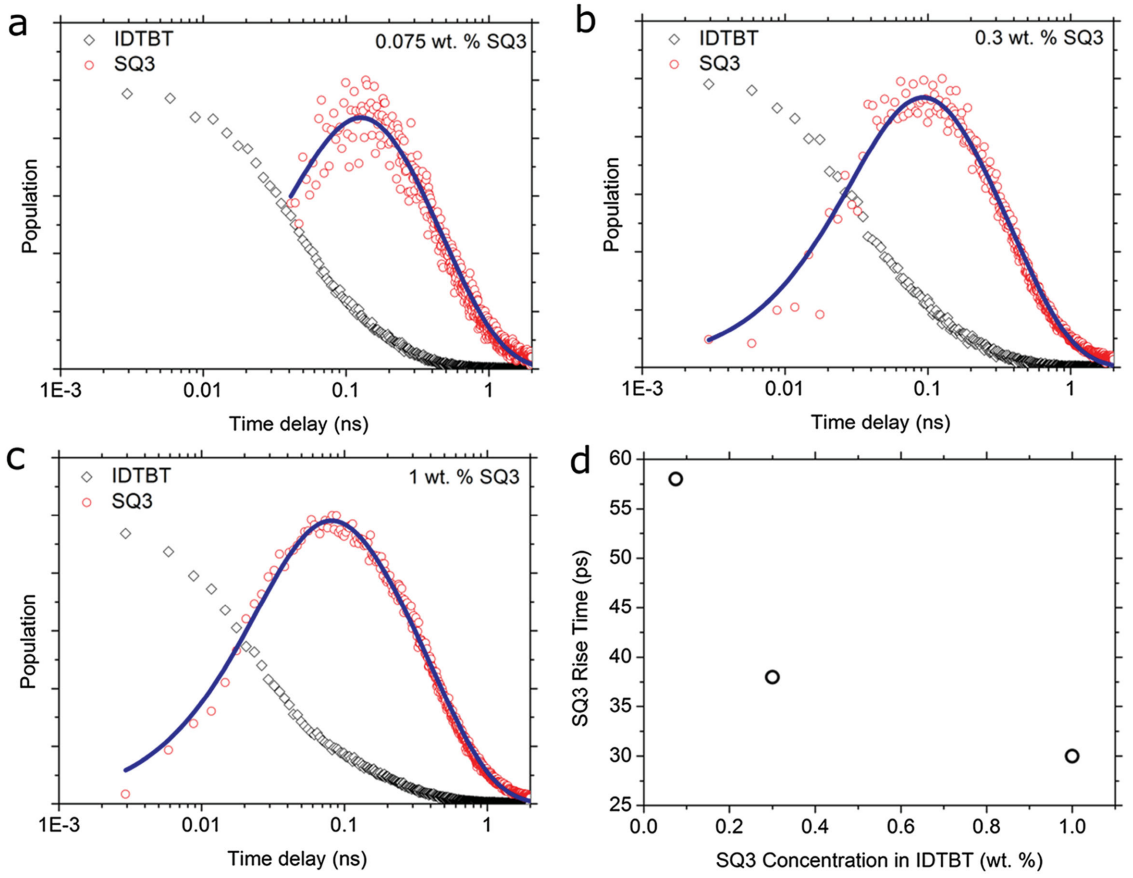

Figure 3. Population dynamics of IDTBT-SQ3 blend films. a–c) Population dynamics for the IDTBT and SQ3 components in blend films containing 0.075, 0.3, and 1 wt. % SQ3. The blue line is the best fit of the population model as described in the main text. These dynamics were deconvoluted from time resolved fluorescence data of the isolated IDTBT component as well as the IDTBT+SQ3 component. d) The rise time of the SQ3 component as extracted from the fitted model. It shows the energy transfer occurs on sub 50 ps timescales of which the rate increases with increasing SQ3 concentration.

the IDTBT population peaks directly after the excitation and decays monotonically, the SQ3 population maximum is delayed by approximately 100 ps consistent with an energy transfer process. The SQ3 population data was fitted with a model describing a rise and fall component of the form

$$P(t) = A\left(1 - e^{-t/\tau_1}\right)e^{-t/\tau_2} \quad (5)$$

where $P(t)$ is the population as a function of time t, A is a constant, and τ_1 is the energy transfer time constant from the IDTBT to the SQ3 and τ_2 is the natural decay rate of the SQ3. From the extracted rise time values in Figure 3d it can be seen that the energy transfer process is fast, occurring on the 50 ps timescale as required for systems with very short exciton lifetimes such as IDTBT.

We incorporated the blend films into organic light emitting diodes to provide a proof of principle without undertaking device optimisation. Six different ratios of IDTBT and SQ3 were chosen, ranging from 0.025 wt. % to 0.3 wt. %. The JV characteristics as well as the peak external quantum efficiency are shown in **Figure 4**a. It can be seen that there is a consistent turn on voltage of 2V and no significant change in current density for the range of concentrations. The EQE peaks at around 7V for all devices and increases from a value of 0.025 % to 0.2 % for 0.3 wt. % SQ3. Figure 4b shows the electroluminescence spectra for the devices and indicates that the emission is dominated by SQ3 even at very low loadings of 0.025 wt. %.

Figure 4c shows the radiance as a function of voltage for a range of SQ3 concentrations. The inset shows that the peak radiance increases from a value of 0.9 to 4.7 W str^{-1} m^{-2} in the highest dye loading concentration. This radiance is comparable to state of the art solution processed inorganic systems.[18,19] Figure 4d combines the EQE, radiance and current densities at two different voltages for all devices. Here we see an increase by a factor of 8 and 5 for the EQE and radiance, respectively. This is facilitated by the lack of a substantial drop in the current densities, which have respective relative values of 0.89 and 0.74 for bias of 4 and 7 V, respectively, compared to the neat devices. It can be seen that the brightness of the neat IDTBT devices is also relatively large at 0.9 W str^{-1} m^{-2} despite its low FQY. This is explained by the OLED experiencing minimal efficiency roll off at high current densities with a $J_{90\%}$ value of 520 mA cm^{-2} (Figure 4e). This value is very high in comparison to other organic systems and is most likely due to the short exciton lifetime of IDTBT which reduces the effects of charge or exciton annihilation. The value of $J_{90\%}$ decreases to 360 mA cm^{-2} for the 0.3 wt. % SQ3 loading, and although still high may be due to the longer lifetime of the SQ3 component. Although

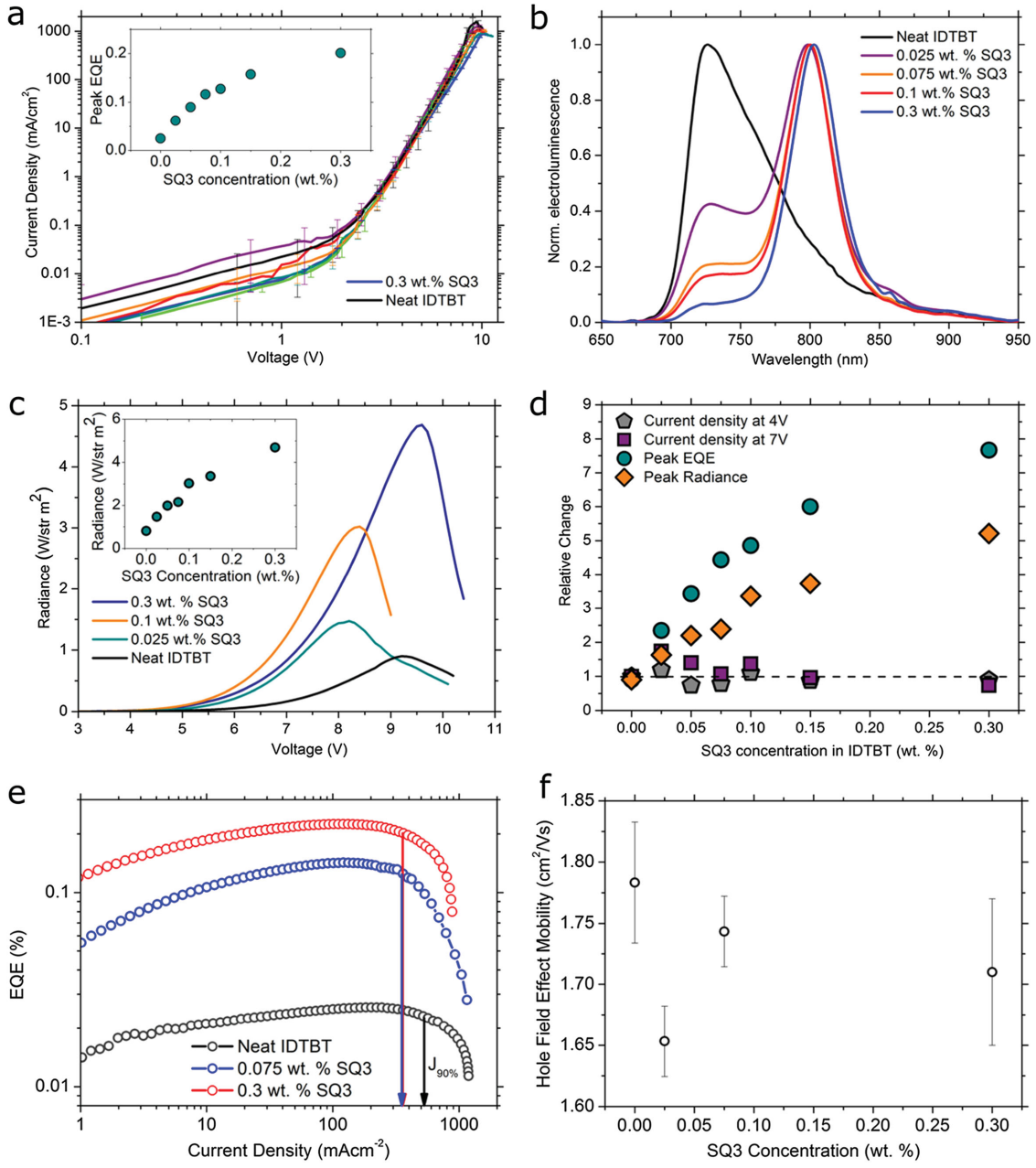

Figure 4. OLED device characteristics of neat and dye-doped active layers. a) *JV* characteristics of neat and dye doped devices. The inset shows the EQE as a function of SQ3 loading. b) The electroluminescence spectra of OLEDs with different SQ3 concentrations. The energy transfer is highly efficient in these devices, evident by the strong SQ3 peak at low dye loadings. c) The radiance as a function of voltage for the devices which peaks between 8 and 10 V for all dye loadings. d) A summary of the relative changes of the device characteristics (EQE, radiance and current density) of dye doped samples as compared to the neat film. It is clear that there is a substantial increase in the radiance and EQE without a significant drop in the current density at 4 and 7 V. e) External quantum efficiency plotted as a function of current density for neat IDTBT as well as blend films containing 0.075 and 0.3 wt. % SQ3. f) Hole mobility values extracted from bottom contact, top gate transistors using neat IDTBT and IDTBT/SQ3 blend films of different concentrations.

no explicit device lifetime tests were carried out in this work, there was no noticeable spectral degradation of the neat or SQ3 doped devices over a period of approximately 10 minutes continuous operation.

To explore the charge transport further, field effect transistors were fabricated and hole mobilities extracted for 3 dye loadings (Supporting Information) and are shown in Figure 4f. It was found that the hole mobilities did not change outside of the device to device variation and had consistently values of around 1.7 $cm^2\ V^{-1}\ s^{-1}$ which is consistent with values reported previously in this group.[12] Interestingly the mobilities achieved here were high despite the lack of any above room temperature annealing step or long range structural order (Supporting Information). This solidifies the argument that long-range

order is not necessary for efficient charge transport.[44] Finally, this gives further evidence that the charge transport is not negatively affected by introducing SQ3 into the thin film.

In conclusion, we have demonstrated the decoupling of electrical performance from electroluminescence in a high mobility polymer semiconductor using efficient RET to a highly fluorescent squaraine dye. This is accomplished by choosing an acceptor molecule with a suitably large spectral overlap with the polymer, which overcomes the low FQY inherent in low bandgap polymers, even in very low concentrations. The resulting bright NIR OLEDs which we give as proof of principle compete with state of the art inorganic devices such as recent perovskite and quantum dot NIR OLEDs. We believe this approach can overcome the current limitations present in all organic systems where a trade-off between charge transport and electroluminescence limits ultrahigh brightness devices. Lastly, there have been a number of reports from the past decade whereby optically pumped lasing has been successfully substituted with RET and has been demonstrated to lower the lasing threshold by orders of magnitude.[45–48] Therefore this approach may be a promising technique to realize an electrically induced population inversion in an organic system.

Experimental Section

Solutions were prepared by dissolving poly(indacenodithiophene-co-benzothiadiazole) (IDTBT provided by Flexink) at 30 mg mL^{-1} in a 75/25 blend of o-dichlorobenzene/chloroform as well as SQ3 at 1 mg mL^{-1} in o-dichlorobenzene. Stock solutions of SQ3 were then prepared by further dissolution in o-dichlorobenzene and these were blended with the IDTBT solution to yield the desired mass ratio. All preparations were carried out in a nitrogen filled glovebox and the solutions were heated at 70 °C on a hotplate for 30 min prior to spinning. Substrates were cleaned by ultrasonication in deionized water, acetone and isopropanol followed by 10 min oxygen plasma treatment. Spin coating was carried out in three stage procedures of 500 rpm for 3 s, 1400 rpm for 120 s, and 5000 rpm for 2 s. This yielded optically thick films of approximately 400 nm.

OLEDs were fabricated by spin coating PEDOT:PSS at 5000 rpm for 30 s on top of an ITO covered substrate and annealing under nitrogen for 10 min at 140°. IDTBT and blend films were spin coated on top using the previous method for spectroscopic characterisation. Calcium was thermally evaporated at a rate of 0.2 Å s^{-1} to a thickness of 20 nm and silver was thermally evaporated at a rate of 0.5 Å s^{-1} to a thickness of 100 nm at a pressure of 1×10^{-6} mbar. Absorption spectroscopy was carried out using a John Woollam M2000 spectroscopic ellipsometer set in transmission mode. Photoluminescence and photoluminescence excitation measurements were performed using an Edinburgh Instruments FLS980 fluorimeter excited with a xenon lamp. Fluorescence lifetime measurements were carried out using time correlated single photon counting in an Edinburgh Instruments LifeSpec -ps where samples were excited with a PicoQuant LDH-P-C 400B 407 nm 10 mW pulsed laser. Alternatively, this was carried out using time correlated single photon counting excited with a femtosecond source. FQY on the blend films was performed using a Thorlabs CPS532 532 nm 4.5 mW continuous wave diode laser. The measurements were carried out under constant nitrogen flow inside of a Labsphere integrating sphere coupled into a spectrometer followed by an Andor iDus DU490A InGaAs detector. PLQE on solutions was measured in an Edinburgh Instruments FLS980 with an integrating sphere. The samples were tested in air without encapsulation and *JV* characteristics were measured using a Keithley 2400 source measure unit. Over a timescale of 24 h there was no observed degradation of the air exposed devices. A calibrated silicon photodiode at a distance of 60 mm from the emission zone was used to determine the photon emission and external quantum efficiency assuming a Lambertian emission profile. EQE and radiance were calculated taking the responsivity of the silicon detector and the photon energy of the OLED emission into account. Electroluminescence spectra were measured using a Labsphere CDS-610 spectrometer and from this combined with photon flux the radiance was calculated.

Supporting Information

Supporting Information is available from the Wiley Online Library or from the author. The data used in this publication can be acessed through the Cambridge University Open Data Repository at https://www.repository.cam.ac.uk/handle/1810/254913.

Acknowledgements

The authors gratefully acknowledge funding from the Engineering and Physical Sciences Research Council (EPSRC) through a Programme Grant No. EP/M005143/1. The authors would like to thank the Doctoral Training Centre in Plastic Electronics EP/G037515/1.K.B. acknowledges financial support by the Deutsche Forschungsgemeinschaft (BR-4869/1-1). The group at Würzburg would like to acknowledge support from the Deutsche Forschungsgemeinschaft (DFG Research Unit FOR 1809) and from the SolTech Initiative of the Bavarian State Ministry of Science, Research and the Arts. D.H. and K.B. would like to thank Dr. Jiři Novak and Jakub Rozbořil (Central European Institute of Technology, Masaryk University, Czech Republic) and Dr. Tom Arnold (Diamond Light Source, Didcot, UK) for assistance during the synchrotron experiment and Diamond Light Source, Didcot, UK for financial support.

Received: February 12, 2016
Revised: March 17, 2016
Published online: May 11, 2016

[1] H. Sirringhaus, *Adv. Mater.* **2014**, *26*, 1319.
[2] Z. Chen, M. J. Lee, R. S. Ashraf, Y. Gu, S. Albert-Seifried, M. M. Nielsen, B. Schroeder, T. D. Anthopoulos, M. Heeney, I. McCulloch, H. Sirringhaus, *Adv. Mater.* **2012**, *24*, 647.
[3] S. Zulkarnaená Bisri, *J. Mater. Chem. C* **2014**, *2*, 2827.
[4] M. Pope, C. E. Swenberg, *Electronic Processes in Organic Crystals and Polymers*, Oxford University Press, Oxford, UK, **1999**.
[5] Z. Hu, A. P. Willard, R. J. Ono, C. W. Bielawski, P. J. Rossky, D. A. Vanden Bout, *Nat. Commun.* **2015**, *6*.
[6] S. Hotta, T. Yamao, *J. Mater. Chem.* **2011**, *21*, 1295.
[7] S. Z. Bisri, K. Sawabe, M. Imakawa, K. Maruyama, T. Yamao, S. Hotta, Y. Iwasa, T. Takenobu, *Sci. Rep.* **2012**, *2*, 985.
[8] S. Z. Bisri, T. Takenobu, Y. Yomogida, H. Shimotani, T. Yamao, S. Hotta, Y. Iwasa, *Adv. Funct. Mater.* **2009**, *19*, 1728.
[9] J. Liu, H. Zhang, H. Dong, L. Meng, L. Jiang, L. Jiang, Y. Wang, J. Yu, Y. Sun, W. Hu, A. J. Heeger, *Nat. Commun.* **2015**, *6*.
[10] R. Englman, J. Jortner, *Mol. Phys.* **1970**, *18*, 145.
[11] J. V Caspar, T. J. Meyer, *J. Phys. Chem.* **1983**, *87*, 952.
[12] D. Venkateshvaran, M. Nikolka, A. Sadhanala, V. Lemaur, M. Zelazny, M. Kepa, M. Hurhangee, A. J. Kronemeijer, V. Pecunia, I. Nasrallah, I. Romanov, K. Broch, I. McCulloch, D. Emin, Y. Olivier, J. Cornil, D. Beljonne, H. Sirringhaus, *Nature* **2014**, *515*, 384.
[13] G. D. Scholes, G. Rumbles, *Nat. Mater.* **2006**, *5*, 683.
[14] M. Shimizu, R. Kaki, Y. Takeda, T. Hiyama, N. Nagai, H. Yamagishi, H. Furutani, *Angew. Chem.* **2012**, *124*, 4171.

[15] L. Yao, S. Zhang, R. Wang, W. Li, F. Shen, B. Yang, Y. Ma, *Angew. Chem. Int. Ed.* **2014**, *53*, 2119.
[16] N. Bamiedakis, J. Beals IV, R. V. Penty, I. H. White, J. V. DeGroot Jr., T. V. Clapp, *IEEE J. Quantum Electron.* **2009**, *45*, 415.
[17] A. Becker, C. Hessenius, K. Licha, B. Ebert, U. Sukowski, W. Semmler, B. Wiedenmann, C. Grotzinger, *Nat. Biotechnol.* **2001**, *19*, 327.
[18] Z.-K. Tan, R. S. Moghaddam, M. L. Lai, P. Docampo, R. Higler, F. Deschler, M. Price, A. Sadhanala, L. M. Pazos, D. Credgington, F. Hanusch, T. Bein, H. J. Snaith, R. H. Friend, *Nat. Nanotechnol.* **2014**, *9*, 687.
[19] L. Sun, J. J. Choi, D. Stachnik, A. C. Bartnik, B.-R. Hyun, G. G. Malliaras, T. Hanrath, F. W. Wise, *Nat. Nanotechnol.* **2012**, *7*, 369.
[20] G. J. Supran, K. W. Song, G. W. Hwang, R. E. Correa, J. Scherer, E. A. Dauler, Y. Shirasaki, M. G. Bawendi, V. Bulovic, *Adv. Mater.* **2015**, *27*, 2311.
[21] O. Fenwick, J. K. Sprafke, J. Binas, D. V Kondratuk, F. Di Stasio, H. L. Anderson, F. Cacialli, *Nano Lett.* **2011**, *11*, 2451.
[22] J. Wang, N. Wang, Y. Jin, J. Si, Z.-K. Tan, H. Du, L. Cheng, X. Dai, S. Bai, H. He, Z. Ye, M. L. Lai, R. H. Friend, W. Huang, *Adv. Mater.* **2015**, *27*, 2311.
[23] G. Qian, Z. Zhong, M. Luo, D. Yu, Z. Zhang, Z. Y. Wang, D. Ma, *Adv. Mater.* **2009**, *21*, 111.
[24] X. Cao, J. Miao, M. Zhu, C. Zhong, C. Yang, H. Wu, J. Qin, Y. Cao, *Chem. Mater.* **2015**, *27*, 96.
[25] G. Tregnago, T. T. Steckler, O. Fenwick, M. R. Andersson, F. Cacialli, *J. Mater. Chem. C* **2015**, *3*, 2792.
[26] W. K. Bae, Y.-S. Park, J. Lim, D. Lee, L. A. Padilha, H. McDaniel, I. Robel, C. Lee, J. M. Pietryga, V. I. Klimov, *Nat. Commun.* **2013**, *4*.
[27] Z. Ning, X. Gong, R. Comin, G. Walters, F. Fan, O. Voznyy, E. Yassitepe, A. Buin, S. Hoogland, E. H. Sargent, *Nature* **2015**, *523*, 324.
[28] S. D. Stranks, G. E. Eperon, G. Grancini, C. Menelaou, M. J. P. Alcocer, T. Leijtens, L. M. Herz, A. Petrozza, H. J. Snaith, *Science* **2013**, *324*, 341.
[29] O. V Mikhnenko, M. Kuik, J. Lin, N. van der Kaap, T.-Q. Nguyen, P. W. M. Blom, *Adv. Mater.* **2014**, *26*, 1912.
[30] T. Förster, *Ann. Phys.* **1948**, *437*, 55.
[31] J. R. Lakowicz, *Principles of Fluorescence Spectroscopy*, Springer Science & Business Media, Singapore **2007**.
[32] K. Cnops, B. P. Rand, D. Cheyns, B. Verreet, M. A. Empl, P. Heremans, *Nat. Commun.* **2014**, *5*, 3406.
[33] B. Stender, S. F. Voelker, C. Lambert, J. Pflaum, *Adv. Mater.* **2013**, *25*, 2943.
[34] J.-S. Huang, T. Goh, X. Li, M. Y. Sfeir, E. A. Bielinski, S. Tomasulo, M. L. Lee, N. Hazari, A. D. Taylor, *Nat. Photonics* **2013**, *7*, 479.
[35] X. Zhang, H. Bronstein, A. J. Kronemeijer, J. Smith, Y. Kim, R. J. Kline, L. J. Richter, T. D. Anthopoulos, H. Sirringhaus, K. Song, M. Heeney, W. Zhang, I. McCulloch, D. M. DeLongchamp, *Nat. Commun.* **2013**, *4*.
[36] W. Zhang, J. Smith, S. E. Watkins, R. Gysel, M. McGehee, A. Salleo, J. Kirkpatrick, S. Ashraf, T. Anthopoulos, M. Heeney, I. McCulloch, *J. Am. Chem. Soc.* **2010**, *132*, 11437.
[37] R. S. Ashraf, B. C. Schroeder, H. A. Bronstein, Z. Huang, S. Thomas, R. J. Kline, C. J. Brabec, P. Rannou, T. D. Anthopoulos, J. R. Durrant, I. McCulloch, *Adv. Mater.* **2013**, *25*, 2029.
[38] C. L. Donley, J. Zaumseil, J. W. Andreasen, M. M. Nielsen, H. Sirringhaus, R. H. Friend, J. S. Kim, *J. Am. Chem. Soc.* **2005**, *127*, 12890.
[39] C. Wuerth, M. Grabolle, J. Pauli, M. Spieles, U. Resch-Genger, *Nat. Protoc.* **2013**, *8*, 1535.
[40] Y. Yang, Y. Zheng, W. Cao, A. Titov, J. Hyvonen, J. R. Manders, J. Xue, P. H. Holloway, L. Qian, *Nat. Photonics* **2015**, *9*, 259.
[41] S. F. Voelker, T. Dellermann, H. Ceymann, M. Holzapfel, C. Lambert, *J. Polym. Sci., Part A: Polym. Chem.* **2014**, *52*, 890.
[42] C. Lambert, T. Scherpf, H. Ceymann, A. Schmiedel, M. Holzapfel, *J. Am. Chem. Soc.* **2015**, *137*, 3547.
[43] C. Lambert, F. Koch, S. F. Völker, A. Schmiedel, M. Holzapfel, A. Humeniuk, M. I. S. Röhr, R. Mitric, T. Brixner, *J. Am. Chem. Soc.* **2015**, *137*, 7851.
[44] R. Noriega, J. Rivnay, K. Vandewal, F. P. V Koch, N. Stingelin, P. Smith, M. F. Toney, A. Salleo, *Nat. Mater.* **2013**, *12*, 1038.
[45] L. Cerdán, E. Enciso, V. Martín, J. Bañuelos, I. López-Arbeloa, A. Costela, I. García-Moreno, *Nat. Photonics* **2012**, *6*, 623.
[46] M. Berggren, A. Dodabalapur, R. E. Slusher, Z. Bao, *Nature* **1997**, *389*, 466.
[47] M. Achermann, M. A. Petruska, S. Kos, D. L. Smith, D. D. Koleske, V. I. Klimov, *Nature* **2004**, *429*, 642.
[48] H. Q. Ye, Z. Li, Y. Peng, C. C. Wang, T. Y. Li, Y. X. Zheng, A. Sapelkin, G. Adamopoulos, I. Hernandez, P. B. Wyatt, W. P. Gillin, *Nat. Mater.* **2014**, *13*, 382.